Open Research Online
The Open University's repository of research publications and other research outputs

Brain endothelial miR-146a negatively modulates T-cell adhesion through repressing multiple targets to inhibit NF-B activation.

Journal Item

For guidance on citations see FAQs.

oro.open.ac.uk

Brain endothelial miR-146a negatively modulates T cell adhesion through repressing multiple targets to inhibit NF-κB activation

Dongsheng Wu[1], Camilla Cerutti[1], Miguel A. Lopez-Ramirez[1,6], Gareth Pryce[2], Josh King-Robson[2], Julie E. Simpson[3], Susanne M. A. van der Pol[4], Mark C. Hirst[1], Helga E. de Vries[4], Basil Sharrack[5], David Baker[2], David K. Male[1], Gregory J. Michael[2], Ignacio A. Romero[1]

[1]Department of Life, Health and Chemical Sciences, Biomedical Research Network, The Open University, Milton Keynes, MK7 6AA, UK.

[2]Center for Neuroscience and Trauma, Blizard Institute, Barts and The London School of Medicine and Dentistry, Queen Mary University of London, London, E1 2AT, UK.

[3]Sheffield Institute for Translational Neuroscience, University of Sheffield, Sheffield, S10 2HQ, UK.

[4]Blood-Brain Barrier Research Group, Molecular Cell Biology and Immunology, VU University Medical Center, Amsterdam, The Netherlands.

[5]Department of Neurology, Sheffield Teaching Hospitals NHS Trust, University of Sheffield, Sheffield, S5 7AU, UK

[6]Department of Medicine, University of California, San Diego, La Jolla, CA 92093, USA

Corresponding **author:** Ignacio A. Romero, Department of Life, Health and Chemical Sciences, Biomedical Research Network, The Open University, Walton Hall, Milton Keynes, MK7 6AA, United Kingdom.

Tel. +44 1908 659467; Fax. +44 1908 654167; Email: nacho.romero@open.ac.uk

Running headline: Brain endothelial miR-146a and T cell adhesion

Abstract

Pro-inflammatory cytokine-induced activation of nuclear factor, NF-κB plays an important role in leukocyte adhesion to, and subsequent migration across, brain endothelial cells (BECs), which is crucial for the development of neuroinflammatory disorders such as multiple sclerosis (MS). In contrast, microRNA-146a (miR-146a) has emerged as anti-inflammatory molecule by inhibiting NF-κB activity in various cell types, but its effect in BECs during neuroinflammation remains to be evaluated. Here, we show that miR-146a was up-regulated in microvessels of MS active lesions and the spinal cord of mice with experimental autoimmune encephalomyelitis (EAE). *In vitro*, TNFα and IFNγ treatment of human cerebral microvascular endothelial cells (hCMEC/D3) led to up-regulation of miR-146a. Brain endothelial over-expression of miR-146a diminished, whereas knock-down of miR-146a augmented, cytokine-stimulated adhesion of T cells to hCMEC/D3 cells, nuclear translocation of NF-κB and expression of adhesion molecules in hCMEC/D3 cells. Furthermore, brain endothelial miR-146a modulates NF-κB activity upon cytokine activation through targeting two novel signaling transducers, RhoA and nuclear factor of activated T cells 5 (NFAT5), as well as molecules previously identified, IL-1 receptor-associated kinase 1 (IRAK1) and TNF receptor-associated factor 6 (TRAF6). We propose brain endothelial miR-146a as an endogenous NF-κB inhibitor in BECs associated with decreased leukocyte adhesion during neuroinflammation.

Introduction

In neuroinflammation such as multiple sclerosis (MS), the blood brain barrier (BBB) becomes compromised with intensive migration of leukocytes into the central nervous system (CNS), contributing to disease pathogenesis.[1] To migrate into the CNS, leukocytes follow a finely regulated sequence of events starting from tethering and rolling along the vessel, then firmly adhering to and emigrating out of the vasculature. Firm adhesion is triggered by chemokines and mediated by interactions between integrins on leukocytes and adhesion molecules on brain endothelial cells (BECs).[2]

Overwhelming evidence highlights that the nuclear factor, NF-κB, drives transcription of cell adhesion molecules, chemokines and pro-inflammatory cytokines.[3] The NF-κB complex consists of a family of dimeric transcription factors comprising RelA (p65), RelB, c-Rel, p50 and p52. The classical pathway involves p50/p65 heterodimers complexed to IκB in unstimulated cells. Upon stimulation, IKKβ mediates the phosphorylation-induced ubiquitination of IκB which frees p50/p65 to translocate to the nucleus to initiate gene transcription.[3] NF-κB also coordinates with other signaling pathways such as RhoA and transforming growth factor-β to modulate the inflammatory response.[4,5] NF-κB has been proposed as a therapeutic target for the treatment of MS,[3] thereby indicating endogenous inhibitors of NF-κB as potential novel therapies.

MicroRNAs (miRNAs) are endogenous non-coding RNAs approximately 22 nucleotides long that pair to the 3'-untranslated region of messenger RNAs and incorporate them into RNA-induced silencing complexes to repress gene expression. Accumulating evidence implicates certain miRNAs in the pathogenesis of MS and experimental autoimmune encephalomyelitis (EAE): miR-155 contributes to the pathogenesis of EAE by modulating T cell differentiation and promoting endothelial

barrier dysfunction,[6,7] whereas brain endothelial miR-125a-5p tightens BBB and prevents leukocyte migration during inflammation.[8]

NF-κB not only initiates the transcription of protein-encoding genes but also drives the precursors to miRNAs which act as feedback modulators of NF-κB.[9] Among them, miR-146a is a NF-κB-dependent gene and down-regulates NF-κB activities by repressing two signal transducers in human monocytes: TNF receptor-associated factor 6 (TRAF6) and IL-1 receptor-associated kinase 1 (IRAK1).[10] Several studies suggest miR-146a as a molecular brake on inflammation, myeloid cell proliferation, and oncogenic transformation.[11] The anti-inflammatory role of miR-146a has been demonstrated in several cell types including monocytes,[10] T cells,[12] astrocytes,[13] human umbilical vein endothelial cells (HUVECs),[14] and human BECs.[15] However, its function in BECs remains to be elucidated. Here we show that miR-146a is up-regulated in cytokine-activated BECs and decreases leukocyte adhesion by inhibiting NF-κB through repressing not only TRAF6 and IRAK1 but also RhoA and nuclear factor of activated T cells 5 (NFAT5).

Materials and Methods

Human brain tissue and primary human T cells

Human brain tissues of MS patients (4 female and 2 male, 34 ~ 88 years old) and control patients (6 male, 35 ~ 84 years old) without neurological diseases were obtained from The UK Multiple Sclerosis Tissue Bank (Imperial College London, London, UK) according to local human ethical guidelines (For clinical information and pathological characterization of MS and control patients please see ref. 7). Primary human T cells were obtained from three healthy donors at VU University Medical Center, Amsterdam, The Netherlands, following the Netherlands human ethical guidelines.[16] Briefly, human CD4+ and CD8+ T cells were purified from peripheral blood mononuclear cells using MACS® magnetic cell sorting kit (Miltenyi Biotec) according to the manufacturer's instructions. CD4+ and CD8+ T cell purity was >96 % as assessed by flow cytometry performed (FACSCalibur™) using CELQuestTM software (BD Biosciences).

Cell lines

The immortalized human brain microvascular endothelial cell line (hCMEC/D3) was cultured on collagen-coated culture flasks or multi-well plates in EGM-2 MV medium supplemented with 2.5% foetal bovine serum (FBS) and growth factors (Lonza, Slough Wokingham, UK).[7] The Jurkat T lymphocyte cell line was a kind gift from Dr V Male (Cambridge University, UK) and cultured in suspension in RPMI1640 (Life Technologies Ltd, Paisley, UK) with 10% FBS.

Induction of experimental autoimmune encephalomyelitis (EAE)

Adult female and male (10 – 12 weeks) Biozzi ABH mice were purchased from Harlan UK Ltd (Bicester, UK). Animals were grouped randomly and maintained on a 12 h: 12 h light: dark cycle and received food and water *ad libitum*. All procedures were approved following ethical review processes in accordance with the Animals (Scientific Procedures) Act 1986 of the UK government. EAE was induced in Biozzi ABH mice with freeze-dried mouse spinal cord homogenate emulsified with complete Freunds adjuvant supplemented as previously described.[7] Animals were monitored daily to assess the development of relapsing–remitting paralysis and scored as follows: 0 = normal; 1 = limp tail; 2 = impaired righting reflex; 3 = hind-limb paresis; 4 = complete hind-limb paralysis and 5 = moribund/death. Two (2/44) animals scored 5 were excluded from the experiments. The EAE status was based on paralytic clinical disease and weight loss/gain as follows: onset of signs: clinical score 1, with weight loss sampled on day 15 post induction; acute-phase paralysis (APP): clinical score 3.5– 4, with weight loss by day 17; recovery: clinical score 3.5–1, with weight gain by day 20; remission one: clinical score 0.5, with weight gain by day 28 after induction. Reporting elements concerning experimental design of EAE experiments relating to the ARRIVE guidelines have been described previously.[7] Data collection and analysis were performed by researchers blinded to the experimental groups.

Laser capture microdissection and isolation of microvessels

Laser capture microdissection (LCM) of MS brain microvessels was used to collect enriched brain endothelium RNA as previously described.[7] Approximately 200 blood vessels were isolated from each case using PixCell II laser capture microdissection system (Arcturus BioScience, Mountain View, CA, USA) and LCM-caps (Applied Biosystems, Warrington, UK). For mouse spinal cords, microvessels

were isolated as previously described.[7] Briefly, EAE or normal ABH mice were perfused with 0.5% bovine serum albumin (BSA) in Hank's balanced solution to rinse out the blood, then the spinal cords were flushed out of vertebral columns. For each replicate, spinal cords of 3 mice in the same group were pooled together to get sufficient amount of RNA and counted as one (total animals used, 9 mice per group), digested with collagenase and dispase (1mg/ml) at 37°C for 1 h, and, finally, homogenized and centrifuged through 25% BSA. The pellet of microvessels underwent a second digestion for 30 min and microvessel fragments were purified and separated from single contaminating cells by passing through a 70 μm size mesh filter. Enrichment of endothelium within the microvessel fraction was examined by quantitative RT-PCR for endothelial markers (*claudin-5, PECAM-1*), astrocyte marker *GFAP* and leukocyte marker *CD45*, as previously described.[7,8]

RNA extraction and quantitative RT-PCR

Total RNA of hCMEC/D3 cells and microvessels isolated from human brain or mouse spinal cords were extracted using TRIzol reagent (Life Technologies Ltd, Paisley, UK). For each sample, 10 ng of total RNA was used for reverse transcription. Expression of miR-146a and U6B small nuclear RNA were measured with TaqMan® MicroRNA Assays Kit (Life Technologies Ltd, Paisley, UK). U6B was used as internal control. QuantiTect SYBR Green PCR kit (Qiagen, Manchester, UK) was used to determine the relative levels of two NF-κB target genes vascular cell adhesion molecule 1 (*VCAM1*) and chemokine C-C motif ligand 2 (*CCL2*). *β-actin* was used as internal control. The primers were 5′-CATTTGACAGGCTGGAGATAGA-3′ and 5′-CTCTTGGTTTCCAGGGACTT-3′ for *VCAM1* (GenBank Accession Number M73255.1), 5′-GGCTGAGACTAACCCAGAAAC3′ and

5′GAATGAAGGTGGCTGCTATGA-3′ for *CCL2* (GenBank Accession Number NM_002982.3), and 5′-GGACCTGACTGACTACCTCAT-3′ and 5′-CGTAGCACAGCTTCTCCTTAAT- 3′ for *β-actin* (NM_001101.3). The method of $2^{-\Delta\Delta CT}$ was used for analysis of the data.[7]

Immunohistochemistry and *in situ* hybridization

   Cryostat sections of lumbar spinal cords from 4% paraformaldehyde-perfused EAE mice at day 10 after EAE induction (D10, n = 5), in the initial acute phase paralysis of EAE with a clinical score of 4 (APP, n = 5), and control mice without EAE induction (n = 5) underwent immunohistochemical staining for endothelial specific marker with rat anti-PECAM-1 monoclonal antibody (1:50, BD Biosciences, Oxford, UK) followed with a secondary goat anti-rat IgG Alexa Fluor 555 (1:400, Life Technologies Ltd, Paisley, UK) and nuclei staining with Hoechst 33342 (Life Technologies Ltd, Paisley, UK). Images were captured using a Leica DMRB fluorescence microscope with a Hamamatsu C4742-95 digital camera and HiPic software (Herrsching, Germany). Then *In situ* hybridization of miR-146a was performed using double-digoxigenin labelled miRCURY LNA™ probe (Exiqon, Vedbaek, Denmark) after proteinase K digestion following the manufacturer's protocol with modification.[7] Briefly slides were treated with 2 µg/ml proteinase K (Roche West Sussex, UK) at 37 °C for 10 min, fixed for 5 min in 4% paraformaldehyde and dehydrated in 70% ethanol. Sections were prehybridised in hybridisation buffer consisting of 50% formamide, 5X saline sodium citrate (SSC) and 100 µg/ml sheared salmon sperm DNA at 52 °C for 30 min. Double-digoxigenin labelled miRCURY LNA™ probe miR-155 oligonucleotide at concentration of 5 nM was hybridised with the sections overnight at 52 °C. A similarly labelled LNA

scrambled oligonucleotide was used as a negative control. Sections were washed

through a series of 5 min washes in 5X to 0.2X SSC at 55°C, incubated overnight

with sheep anti-digoxigenin antibody conjugated with alkaline phosphatase (1:1000,

Roche West Sussex, UK), then incubated in NBT/BCIP (Roche West Sussex, UK)

and levamisole (Vector Labs, Peterborough, UK) at 30 °C, then washed in KTBST

(50 mM Tris HCl pH 7.5, 150 mM NaCl, 20 mM KCl, 0.5% Tween-20) for 1 to 6 h to

reduce the background signal. Sections were re-stained in Hoechst 33342. NBT/BCIP

precipitate was photographed using a Nikon Eclipse 80i fluorescence microscope with

a MBF CX9000 digital camera and PictureFrame software.

Cell transfection

30 nM of Pre-miR-146a were transfected into hCMEC/D3 cells using siPORT

Amine transfection agent (Life Technologies Ltd, Paisley, UK), whereas 60 nM of

miR-146a inhibitor (Anti-miR-146a) and siGENOME SMARTpool siRNAs for

human RelA, IRAK1, TRAF6, STAT1, ROCK1, RhoA, and NFAT5 (ThermoFisher

Scientific, Epsom, UK) were transfected into cells using Lipofectamine 2000 (Life

Technologies Ltd, Paisley, UK). Non-targeting scrambled Pre-miR, Anti-miR or

siRNA control pools was used as negative controls respectively. Cy3™ dye-Labeled

Pre-miR or Anti-miR Negative Control #1 (Life Technologies Ltd, Paisley, UK),

siGLO Red Transfection Indicator (ThermoFisher Scientific, Epsom, UK) was used

for analysing transfection efficiency.

Leukocyte adhesion assay under shear flow

Jurkat T cell and primary human T cell adhesion assay was performed as

previously described with modification.[17,18] Briefly, hCMEC/D3 cells were grown on

collagen-coated ibidi μ-Slide VI$^{0.4}$ 6 channel slides (ibidi GmbH, Martinsried, Germany) until confluence. Primary human T cells were activated by 48 h stimulation with IL-2 (10 ng/ml) and phytohemagglutinin (1 μg/ml). Then Jurkat T cells or activated primary human T cells (2 x 10^6/ml) were labelled with 5 mM CMFDA (5-chloromethylfluorescein diacetate, Life Technologies Ltd, Paisley, UK) and were allowed to flow through the channel and accumulate for 5 min at low shear stress (0.5 dyn/cm^2). Shear stress (τ) was calculated according to $\tau = 176.1\, \eta\Phi$ ($\eta = 0.01$, $\Phi =$ volumetric flow rate). Images were recorded at one frame per second with an inverted time-lapse fluorescence microscope (Olympus IX70, Tokyo, Japan) by using Image Pro Plus software (Media Cybernetics Inc., Bethesda, USA). Then culture medium was pulled through the channel at a physiological shear stress (1.5 dyn/cm^2) for 1 min to wash away leukocytes which were not firmly adhered to endothelium. Under physiological shear stress, images were taken randomly from, at least 5 fields per channel (640 x 480 μm^2/field). Firmly adherent Jurkat T cells were then counted using Image Pro Plus software.

Immunocytochemistry

hCMEC/D3 cells grown on glass coverslips coated with collagen were fixed with 4% paraformaldehyde and permeabilized with methanol and acetone at -20°C for 10 and 1 min respectively, then incubated with rabbit anti-NF-κB p65 (1:100, Cell Signaling Technology Inc. Danvers, MA, USA) followed by goat anti-rabbit IgG Alexa Fluor 488 (1:400, Life Technologies Ltd, Paisley, UK). Cell nuclei were stained using Dapi Fluoromount-G (SouthernBiotech, Birmingham, Alabama, USA). Images were captured with a Zeiss Axiophot fluorescent microscope. Number of cells with nuclear staining of NF-κB p65 was expressed as percentage of total cell numbers

demonstrated by DAPI, for each experiment and each condition performed with duplicates, at least 100 cells were counted in 3 – 6 randomly selected fields.

Western blot analysis

Cell lysates were separated by 10% (20% for RhoA) SDS-PAGE gels and transferred onto nitrocellulose membranes (Amersham, Buckinghamshire, UK), probed with rabbit anti-IRAK1 or TRAF6 or RelA or ROCK1 (1:1000, Cell Signaling Technology, Danvers, MA, USA), or rabbit anti-NFAT5 (1:1000, Thermo Scientific, Northumberland, UK) or STAT1 (1:500, Santa Cruz Biotechnology, Inc., Dallas, Texas, USA), or mouse anti-RhoA (1:100, Cytoskeleton, Inc. Denver, CO, USA), or mouse anti-VCAM1 (1:100, R&D Systems Europe Ltd, Abingdon, UK), or mouse anti-β-actin (1:5000 Sigma, Dorset, UK), followed with horseradish peroxidise-conjugated goat anti-rabbit IgG (1:3000; Life Technologies Ltd, Paisley, UK) or anti-mouse IgG (1:3000 for RhoA, 1:14000 for β-actin; Pierce Biotechnology, Cheshire, UK). Immunoblots were then developed by enhanced chemiluminescence detection (ECL, Amersham, Buckinghamshire, UK).

Lentiviral transduction of 3' UTR reporter vectors and luciferase assay

The luciferase reporter lentiviral vector constructs containing the puromycin resistance gene and the luciferase gene from the firefly Photinus pyralis with the 3'untranslated region (UTR) of RhoA (1061 bases), NFAT5 (5'-2100 bases) (Applied Biological Materials Inc., British Columbia, Canada) were used to transduce hCMEC/D3 cells with a multiplicity of infection of 3. Mutated 3' UTR versions of putative target genes were obtained by replacing the corresponding miR-146a target sites with AAGA using site-directed mutagenesis. 24 h after transduction, cells were

transfected with Pre-miR-146a or scrambled Pre-miR. 72 h later, luciferase activity was quantified using the Steady-Glo® Luciferase assay system (Promega, Madison, WI, USA) and luminescence was determined using the FLUOstar OPTIMA plate reader (BMG LABTECH GmbH, Ortenberg, Germany).

Statistical analysis

All values are presented as means ± SEM. Student paired *t* test was used for human MS samples, Jurkat T cell or primary human T cell adhesion assay. Student *t* test was used for 3' UTR luciferase assay. For other experiments, one-way ANOVA (analysis of variance) was used for single time point experiments and posthoc with Bonferroni correction for multiple comparisons on SPSS software. Two-way ANOVA was used for multiple time point experiments. Statistical significance was considered if $P < 0.05$.

Results

Neuroinflammation induces up-regulation of CNS endothelial miR-146a

To elucidate the role of endothelial miR-146a in BBB dysfunction in neuroinflammatory diseases such as MS, we first characterized its expression in human brain microvessels of MS lesions, isolated by laser capture microdissection. In comparison to normal appearing white matter, cerebral microvascular miR-146a increased approximately 1.5 fold in the active lesions of MS (Figure 1A). We then examined the temporal expression pattern of miR-146a in the spinal cord microvasculature of EAE mice, isolated by enzyme digestion. The enrichment of endothelium was confirmed, as previously reported by our lab,[7] by high gene expression levels of endothelial specific markers (*claudin-5, PECAM-1*) and by low expression of astrocyte marker *GFAP* and leukocyte marker *CD45*, compared to the reference gene *β-actin*. Mice at initial acute-phase paralysis of EAE (EAE-APP) with a clinical score of 4 showed an 8-fold increase of miR-146a in the microvessels of the spinal cord compared to normal control animals (Figure 1B). The level of miR-146a returned back to basal levels during EAE-remission stage. We further demonstrated, via *in situ* hybridization, the abundant expression of miR-146a in the lumbar spinal cord of EAE-APP mice, and its co-localization with the endothelial maker PECAM-1 (Figure 1C). In non-EAE control mice or in EAE mice at day10 (D10) after immunization (prior to onset of signs), endothelial expression of miR-146a was not detectable or very low, respectively (Figure 1C). In cultured human brain endothelial hCMEC/D3 cells, an *in vitro* BBB model, tumor necrosis factor alpha (TNFα) and interferon gamma (IFNγ) (1 ng/ml each) up-regulated the expression of miR-146a at 6 and 24 h by 4 fold of that in non-stimulated control cells and this increase was still largely maintained (~3 fold) by 48 h post-cytokine stimulus (Figure 1D). These

results indicate that inflammatory mediators induce a tightly spatial and temporal expression of miR-146a, thereby suggesting an important role at brain endothelium in affected areas during neuroinflammation.

Brain endothelial miR-146a partially prevents cytokine-stimulated leukocyte adhesion

As miR-146a levels increase in brain endothelium during neuroinflammation, we then further investigated the role of brain endothelial miR-146a in BBB dysfunction, particularly on leukocyte adhesion to brain endothelium *in vitro*. We firstly manipulated the levels of miR-146a in hCMEC/D3 cells grown on 6-channel slides by transfection with Pre-miR-146a or Anti-miR-146a to increase or decrease the expression of miR-146a respectively (Supplementary Figures 1A and B). For all experiments, over 90% transfection efficiency was consistently achieved (Supplementary Figure 1C). At day 1 post-transfection, cells were treated with 1 ng/ml TNFα and IFNγ for 24 h and exposed to CMFDA-labelled Jurkat T cells for 5 min at 0.5 dyn/cm^2 to mimic the blood flow in the microvasculature (Supplementary Videos A-C). Jurkat T cells adhered to endothelial cells were analysed after flushing away non-adhered cells at 1.5 dyn/cm^2. We observed that ectopic expression of miR-146a or inhibition of basal miR-146a by Anti-miR-146a did not affect Jurkat T cell adhesion to non-stimulated hCMEC/D3 monolayers (Figures 2A and B). In contrast, stimulation of endothelium with 1 ng/ml TNFα and IFNγ for 24 h induced increase in Jurkat T cell adhesion by around 10 fold, under flow condition, when compared to non-treated cells (Figures 2A and B). Furthermore, over-expression of miR-146a in brain endothelium partially prevented Jurkat T cell adhesion to cytokine-activated

16

hCMEC/D3 cells by ~21% (Figure 2A; Supplementary Videos B and C). Preventing

cytokine-induced increase in miR-146a resulted in augmented Jurkat T cell adhesion

by ~39% (Figure 2B). Similarly, over-expression of miR-146a in brain endothelium

partially prevented primary human T cell adhesion to cytokine-activated hCMEC/D3

cells by ~17% (Figures 2C). Altogether, these results indicate TNFα and IFNγ induce

increase of brain endothelial miR-146a that negatively modulates Jurkat T cell

adhesion.

miR-146a modulates brain endothelial NF-κB activation

The critical role of NF-κB in leukocyte adhesion to and migration across endothelium

is well established, so we next wanted to investigate whether miR-146a modulates

NF- κB activity in brain endothelium. Following immunostaining of NF-κB p65, our

results show that 1 ng/ml of TNFα and IFNγ induced nuclear translocation of NF-κB

p65 in hCMEC/D3 cells which peaked at 0.5 h and was largely sustained from 6 to 24

h (Figure 3A-C). Over-expression of miR-146a decreased cytokine-induced NF-κB

p65 nuclear translocation at all three time points, by 8%, 20% and 10% at 0.5, 6 and

24 h, respectively, compared to their scrambled controls (Figure 3A and B). By

contrast, miR-146a knock-down enhanced cytokine-induced NF-κB p65 nuclear

translocation by 3%, 7% and 15% over that of scrambled control at 0.5, 6 and 24 h,

respectively (Figure 3C). In line with a previous report on the role of NF-κB on

monocyte adhesion to umbilical vein endothelium,[18] we confirmed that knock-down

of RelA (NF-κB p65) via small interference RNA (Figure 3D) decreased Jurkat T cell

adhesion to cytokine-activated brain endothelium by 67% in comparison with its

scrambled control (Figure. 3E). These results suggest that cytokine-induced miR-146a

up-regulation in brain endothelium negatively regulated upstream activators of NF-κB signaling.

miR-146a targets IRAK1 and TRAF6 in brain endothelium

As microRNAs regulate cellular processes and cell signaling through silencing target molecules, using different online databases (microRNA.org, MiRanda and TargetScan), we identified 4 potential target genes for miR-146a with known NF-κB regulatory activity, STAT1, ROCK1, RhoA and NFAT5, in addition to the well-known miR-146a targets, IRAK1 and TRAF6. Indeed, these two genes have already been validated as targets of miR-146a in several cell types including monocytes, T cells and astrocytes,[10,12,13] and are involved in the regulation of NF-κB activity and expression of NF-κB target genes such as *VCAM1* and *TNFα*.[13,14] We transfected hCMEC/D3 cells with Pre-miR-146a or scrambled control, then treated cells with 1 ng/ml TNFα and IFNγ for 0.5, 6 and 24 h. In the control conditions, cytokines increased IRAK1 (by 1.25 fold over untreated control) at 0.5 h, with levels decreasing considerably (by 25 ~ 40%) at later time points (Figures 4A and B). In contrast, TRAF6 expression levels were increased at all three time points by cytokine treatment (1.1 – 1.4 fold of untreated control) (Figures 4A and C). We show that ectopic expression of miR-146a suppressed levels of IRAK1 and TRAF6 (Figures 4A-C), in either untreated or cytokine-treated hCMEC/D3 cells at all three time points by Western blot analysis. Moreover, knock-down of the expression of IRAK1 or TRAF6, alone or in combination, via small interference RNAs (siIRAK1, siTRAF6) (Supplementary Figures 3A and B), significantly decreased cytokine-induced leukocyte adhesion (Figures 4D-F) and this effect was associated with decreased nuclear translocation of NF-κB (Figure 4G). We did not observe synergistic or

additive effects when knock-down of TRAF6 and IRAK1 was conducted simultaneously by small interference RNAs.

Two additional potential miR-146a targets, STAT1 and ROCK1, have been respectively validated in prostate carcinoma cells[19] and T_{reg} cells.[20] However, in brain endothelium, miR-146a suppressed neither STAT1 nor ROCK1 protein expression (Supplementary Figure 2).

miR-146a targets NFAT5 and RhoA in brain endothelium

We further investigated two novel potential targets for miR-146a in brain endothelium that have not previously been validated: RhoA and NFAT5. We transfected hCMEC/D3 cells with Pre-miR-146a, then treated them with 1 ng/ml TNFα and IFNγ for 0.5, 6 and 24 h. In controls, cytokines increased NFAT5 (around 20% more than untreated control) from 0.5 to 6 h, after which levels decreased slightly (Figures 5A and B). In contrast, RhoA levels decreased by 20% at 6 h, then increased by 20% at 24 h (Figures 5A and C). We show that ectopic expression of miR-146a suppressed levels of both NFAT5 and RhoA (Figures 5A-C), in either untreated or cytokine-treated hCMEC/D3 cells at all three time points by Western blot analysis. Moreover, knock-down of NFAT5 or RhoA expression using small interference RNAs (siNFAT5, siRhoA) (Supplementary Figure 3C), significantly decreased leukocyte adhesion to cytokine-activated brain endothelium by 33% or 37% respectively (Figures 5D and E). siNFAT5 down-regulated nuclear translocation of NF-κB by15%, 14% and 11% at 0.5, 6 and 24 h, respectively, compared to their scrambled controls, while siRhoA decreased nuclear translocation of NF-κB by 7% at all three time points (Figure 5F). Furthermore, in hCMEC/D3 cells transduced with lentiviral luciferase reporter vectors containing the 3' UTR of RhoA or NFAT5, over-expression of miR-

146a significantly decreased luciferase activity by 50% and 30% respectively in comparison with scrambled controls, but no decrease was detected in cells transduced with lentiviral luciferase reporter vector containing mutated 3' UTR versions of either RhoA or NFAT5 (Figure 5G). These results demonstrated that miR-146a play a key role in modulating NF-κB activity by repressing multiple cytokine-effectors.

miR-146a inhibits expression of NF-κB-target genes in brain endothelium

As miR-146a modulates NF-κB activation by repressing multiple targets, we then examined its effect on the mRNA and protein expression of two NF-κB-target genes: *VCAM1* and *CCL2*, which are key players in leukocyte adhesion to endothelium. In cytokine-treated hCMEC/D3 cells, *VCAM1* and *CCL2* mRNA levels increased by 70- and 50-fold over that of untreated cells, respectively, whereas over-expression of miR-146a by transfection with Pre-miR-146a decreased the cytokine-induced levels of *VCAM1* and *CCL2* by 50% (Figure 6A). In contrast, decreased expression of miR-146a by transfection with Anti-miR-146a increased the level of *VCAM1* mRNA in cytokine-activated hCMEC/D3 cells (Figure 6B). *CCL2* mRNA levels were also increased by transfection with Anti-miR-146a but did not reach statistical significance. Consistently, knock-down of NFAT5 and RhoA by siRNA decreased the transcription levels of *VCAM1* and *CCL2* by 50% in cytokine-stimulated cells (Figure 6D), whereas siIRAK1 and siTRAF6 did not markedly alter the levels of *VCAM1* and *CCL2* mRNA (Figure 6C). We further examined the protein levels of VCAM1 in hCMEC/D3 cells transfected with Pre-miR-146a or with siRNA for its target molecules. Cytokines increased the level of VCAM1 protein, whereas ectopic expression of miR-146a significantly decreased cytokine-induced levels of VCAM1 protein (Figure 6E). In addition, siRNA-mediated knock-down of IRAK1, TRAF6,

RhoA and NFAT5 significantly decreased VCAM1 protein levels in cytokine-activated cells (Figures 6F-H), which is in line with that down-regulated by siRelA (Figure 6I).

Taken together, these results indicate that cytokine-induced increase in brain endothelial miR-146a negatively regulates NF-kB activation via repression of multiple targets upstream of NF-kB signaling, highlighting its anti-inflammatory role in brain endothelium.

Discussion

miR-146a has been demonstrated as a NF-kB inhibitor in several cell types other than brain endothelium. In this study we provide evidence that brain endothelial miR-146a represses multiple targets: NFAT 5, RhoA, IRAK1 and TRAF6, to inhibit NF-kB activity, and subsequently negatively modulate leukocyte adhesion (Figure 7).

In vivo, we have shown that miR-146a is significantly up-regulated in isolated microvessels of MS active lesion and of spinal cords of mice during EAE-APP. In the spinal cords of EAE mice, we further confirmed the expression of miR-146a in endothelium by *in situ* hybridization combined with immunohistochemistry. The expression of miR-146a starts to appear prior to the onset of signs, reaches high levels during EAE-APP when pro-inflammatory cytokines are extensively produced,[1-3] and maximum cell infiltration is occurring around the vasculature, and draws back to baseline at remission when BBB dysfunction is restored and with minimal cell infiltration.[7] This observation is in line with the increased expression of miR-146a detected in active MS lesion and in cytokine-treated astrocytes.[21] We also demonstrate that miR-146a is up-regulated in cytokine-activated cultured BECs, where NF-κB activation occurs earlier than miR-146a up-regulation. It is possible that miR-146a is transcribed upon onset of inflammation by NF-κB and levels increase during acute stage of inflammatory conditions in order to resolve neuroinflammation (Figure 7). It is thus reasonable to predict that miR-146a may act as an anti-inflammatory microRNA in astrocytes and brain endothelial cells as they form a functional neurovascular unit to maintain the integrity of BBB.[22]

NF-κB has been shown to be a central player in several autoimmune diseases such as MS.[3] The NF-κB pathway fulfils diverse roles in development, maturation, activation and proliferation of lymphocytes, and in regulating pro-inflammatory and anti-inflammatory function of dendritic cells and macrophages.[3] Brain endothelial transcripts regulated by NF-κB may include not only miR-146a[11] but also nitric oxide synthases, pro-inflammatory cytokines, chemokines and cell adhesion molecules.[3] In cultured brain,[23] umbilical vein[18] or retina[24] endothelial cells, inhibition of NF-κB activity reduces TNFα-induced permeability and/or leucocyte migration. *In vivo*, reagents used to block NF-κB activity can reduce the incidence of disease and clinical score of EAE.[25] Here we show that endothelial miR-146a diminishes both Jurkat T cell and primary T cell adhesion to BECs, an effect that is associated with a decrease in NF-kB nuclear translocation. Similar effects on leukocyte adhesion to endothelium have been observed with NF-kB inhibitors such as MG-132, adenoviral IκB,[18,23] and small interference for RelA (Figure 3D). The effect of miR-146a on NF-kB nuclear translocation was relatively small at the very early time point. This may result from the fine tuning properties of miRNAs[7] and also the characteristic of NF-kB nuclear translocation that peaks at early time points and then resolves gradually (Figure 3A). Furthermore the relative large effect of miR-146a at later time points may result from additive effects of NF-kB induced negative feedback regulators such as Bcl3 and IκB.[3] Nevertheless, the general effect of endothelial miR-146a on leukocyte adhesion to BECs through inactivating NF-κB is evident. Even though MS is regarded as a T lymphocyte-dependent chronic inflammatory disease, other cells like B cells, dendritic cells, macrophages and CNS resident glia also contribute to the pathogenesis of disease.[3] The effects of endothelial expression of miR-146a on other cell types including various subsets of T cells remain to be explored.

It has been demonstrated that miR-146a negatively modulates NF-κB through down-regulating TRAF6 and IRAK1.[10-13] In BECs, we also demonstrated that miR-146a repressed translation of TRAF6 and IRAK1 in response to TNFα and IFNγ. Knock-down of TRAF6 and IRAK1 either individually or simultaneously show similar effects as miR-146a on Jurkat T cell adhesion and nuclear translocation of NF-κB, although simultaneous knock-down of both proteins together did not result in synergistic effects. TRAF6 and IRAK1 have been mainly associated with IL-1β signal transduction leading to NF-κB activation,[10-13] but several reports demonstrate a role for these two signalling molecules in TNFα-induced NF-κB activation.[26-28] In addition, an endogenous IL-1 inhibitor, IL1 receptor antagonist (IL-1RA), blocked IL-1β- but not TNFα/INFγ-induced NF-kB activation and Jurkat T cell adhesion to BECs (Supplementary Figure 4), indicating that TNFα-induced IL-1 expression was not involved in the miR-146a-mediated TRAF6 and/or IRAK1 inhibition on NF-κB activity. This effect is however limited, suggesting the involvement of other NF-kB modulators targeted by miR-146a that are specific for TNFα and IFNγ. However, levels of another two known miR-146a targets, ROCK1 (ref. 19) and STAT1 (ref. 20), were not affected by miR-146a over-expression, suggesting tissue-specific actions of miRNAs.

We also identified another two novel miR-146a targets known to modulate NF-kB activity, NFAT5 and RhoA. NFAT5 together with NFAT1 – 4 belong to the Rel family, sharing 15 – 17% identity with p50 in the Rel homology region.[29] Most reports on NFAT5 refer to its transcriptional activity in the context of hypertonicity.[29] However its role in inflammation is only beginning to emerge, with evidence that pro-

inflammatory cytokines TNFα, IL-1, IL-6, IL-18, and chemokines such as CXCL8, CCL2 and CCL5 are transcriptional targets of NFAT5 in various cell types and under various inflammatory stimuli.[29,30] Furthermore there appears to be cross-talk between NFAT5 and NF-κB[30] or Wnt/β-catenin[31], where the latter is important for BBB development. Accumulating evidence suggests the onset of local or systemic hyperosmolality during the course of various inflammatory disorders such as diabetic microvascular lesions and inflammatory bowel disease. Recently it has been reported that a high salt diet leads to a more severe EAE clinical outcome through an effect relying on p38-MAPK and NFAT5-dependent Th17 development.[32] We provide further evidence that NFAT5 is involved in the activation of cerebral endothelium by cytokines, particularly concerning regulation of NF-κB activation and T cell adhesion.

RhoA, Cdc42 and Rac1 are members of the Rho family of small GTPases. Endothelial Rho has been shown to play a crucial role in leukocyte migration across of BECs either by modulating the cytoskeleton to embrace leukocyte by promoting docking structures[33] or by acting as an intercellular adhesion molecule-1 signal transducer.[34] In other endothelium (mostly HUVECs), RhoA has been shown to modulate expression of cytokines, adhesion molecules and chemokines via Rho/ROCK/(actin cytoskeleton)/NF-kB signaling cascade.[4] Rho family members and their exchange factors Dbl, Ost, and Vav potently activate NF-kB, though other transcription factors such as the activating protein-1 (AP-1) family member c-Jun may also coordinately act together to modulate NF-kB activities. Our results demonstrating a link between miR-146a and RhoA are in agreement with the role of RhoA in NF-kB activation and leukocyte adhesion to endothelium.

We have also examined the levels of adhesion molecules down-regulated by miR-146a (Figure 6), because of the well-documented observation that NF-κB initiates adhesion molecule expression and chemokine production in multiple cell types including brain endothelial cells.[3] It seems a reasonable assumption therefore, that cerebral endothelial miR-146a may regulate signal transducers for NF-κB activation posttranscriptionally, thereby leading to decreased expression of NF-κB transcriptional targets. Indeed, our results are in line with those obtained in HUVECs, where manipulating levels of miR-146 had a significant indirect effects on transcription of intercellular adhesion molecule-1 (ICAM1), VCAM1, E-selectin, CCL2, whereas these effects are not only due to targeting of NF-κB activation but also other signaling molecules such as mitogen-activated protein kinase/early growth response pathway and AP-1 signaling.[15] Unexpectedly, we also observed that siIRAK1 and/or siTRAF6 decreased VCAM1 protein levels without affecting its corresponding mRNA levels. It is possible that the role of these two signalling proteins in the inflammatory activation of brain endothelial cells induced by cytokines is a complex process and that, in addition to their role in NF-kB-mediated transcriptional activation, IRAK1 and TRAF6 may regulate inflammatory molecules such as VCAM1 at the post-translational level. As an example, IL-1 activates a translational control mechanism that modulates expression of a group of genes, including IL-6, via IRAK1[35]. Alternatively, combination of pro-inflammatory cytokines increases the half-life of VCAM1 mRNA[36], and TRAF6 and IRAK1 actively regulate the ubiquitin-proteasome system.[37] It is thus conceivable that VCAM1 protein turnover is affected by ablation of IRAK1 and/or TRAF6 in the absence of apparent changes of VCAM1 mRNA levels by a mechanism that remains to be determined.

In summary, we have delineated further the underlying mechanisms through which miR-146a affects T cell adhesion to human brain endothelium by identifying two novel targets NFAT5 and RhoA, and we have demonstrated the role of IRAK1 and TRAF6, two signalling molecules usually associated with IL-1R and Toll like receptor responses, in brain endothelial activation by TNFα and IFNγ, we have characterized the temporal and spatial expression of miR146a in CNS endothelium in MS active lesions, EAE model and cultured brain endothelium. Since the complex signaling networks appear to control inflammation progression,[28,38] it is unlikely that rational therapeutic strategies should focus on modulating the activity of one signaling molecule. Indeed the emerging role of miRNAs in directly regulating complex signaling networks involved in inflammation such as cell adhesion molecules[39,40] by targeting the expression of several genes makes them suitable therapeutic targets for neuroinflammatory disorders. The limited increase of miR-146a in MS brain endothelium further stresses the necessity to increase miR-146a through therapeutic manipulation to counteract inflammatory responses, thereby potentially preventing the progression of MS pathogenesis.

Conflict of interest: The authors declare no conflict of interest.

Supplementary information is available at the Journal of Cerebral Blood Flow &

Metabolism website – www.nature.com/jcbfm

References

1. Larochelle C, Alvarez JI, Prat A. How do immune cells overcome the blood-brain barrier in multiple sclerosis? *FEBS Lett* 2011; **585**: 3770-3780.

2. Rossi B, Angiari S, Zenaro E, Budui SL, and Constantin G. Vascular inflammation in central nervous system diseases: adhesion receptors controlling leukocyte-endothelial interactions. *J Leukoc Biol* 2011; **89**: 539-556.

3. Yan J, Greer JM. NF-kappa B, a potential therapeutic target for the treatment of multiple sclerosis. *CNS Neurol Disord Drug Targets* 2008; **7**: 536-557.

4. Shimada H, Rajagopalan LE. Rho kinase-2 activation in human endothelial cells drives lysophosphatidic acid-mediated expression of cell adhesion molecules via NF-kappaB p65. *J Biol Chem* 2010; **285**: 12536-12542.

5. Freudlsperger C, Bian Y, Contag Wise S, Burnett J, Coupar J, Yang X *et al*. TGF-beta and NF-kappaB signal pathway cross-talk is mediated through TAK1 and SMAD7 in a subset of head and neck cancers. *Oncogene* 2013; **32**: 1549-1559.

6. O'Connell RM, Kahn D, Gibson WS, Round JL, Scholz RL, Chaudhuri AA *et al*. MicroRNA-155 promotes autoimmune inflammation by enhancing inflammatory T cell development. *Immunity* 2010; **33**: 607-619.

7. Lopez-Ramirez MA, Wu D, Pryce G, Simpson JE, Reijerkerk A, King-Robson J *et al*. MicroRNA-155 negatively affects blood-brain barrier function during neuroinflammation. *FASEB J* 2014; **28**: 2551-2565.

8. Reijerkerk A, Lopez-Ramirez MA, van Het Hof B, Drexhage JA, Kamphuis WW, Kooij G *et al*. MicroRNAs regulate human brain endothelial cell-barrier

function in inflammation: implications for multiple sclerosis. *J Neurosci* 2013; **33**: 6857-6863.

9. Boldin MP, Baltimore D. MicroRNAs, new effectors and regulators of NF-kappaB. *Immunol Rev* 2012; **246**: 205-220.

10. Taganov KD, Boldin MP, Chang KJ, Baltimore D. NF-kappaB-dependent induction of microRNA miR-146, an inhibitor targeted to signaling proteins of innate immune responses. *Proc Natl Acad Sci USA* 2006; **103**: 12481-12486.

11. Boldin MP, Taganov KD, Rao DS, Yang L, Zhao JL, Kalwani M *et al*. miR-146a is a significant brake on autoimmunity, myeloproliferation, and cancer in mice. *J Exp Med* 2011; **208**: 1189-1201.

12. Yang L, Boldin MP, Yu Y, Liu CS, Ea CK, Ramakrishnan P *et al*. miR-146a controls the resolution of T cell responses in mice. *J Exp Med* 2012; **209**: 1655-1670.

13. Iyer A, Zurolo E, Prabowo A, Fluiter K, Spliet WG, van Rijen PC *et al*. MicroRNA-146a: a key regulator of astrocyte-mediated inflammatory response. *PLoS One* 2012;**7**: e44789.

14. Cheng HS, Sivachandran N, Lau A, Boudreau E, Zhao JL, Baltimore D *et al*. MicroRNA-146 represses endothelial activation by inhibiting pro-inflammatory pathways. *EMBO Mol Med* 2013; **5**: 1017-1034.

15. Zhang L, Chopp M, Liu X, Teng H, Tang T, Kassis H *et al*. Combination therapy with VELCADE and tissue plasminogen activator is neuroprotective in aged rats after stroke and targets microRNA-146a and the toll-like receptor signaling pathway. *Arterioscler Thromb Vasc Biol* 2012; **32**: 1856-64.

16. Kooij G1, Kroon J, Paul D, Reijerkerk A, Geerts D, van der Pol SM *et al*. P-glycoprotein regulates trafficking of CD8(+) T cells to the brain parenchyma. *Acta Neuropathol* 2014; **127**: 699-711.

17. Steiner O, Coisne C, Engelhardt B, Lyck R. Comparison of immortalized bEnd5 and primary mouse brain microvascular endothelial cells as in vitro blood-brain barrier models for the study of T cell extravasation. *J Cereb Blood Flow Metab* 2011; **31**: 315-327.

18. Weber KS, Draude G, Erl W, de Martin R, Weber C. Monocyte arrest and transmigration on inflamed endothelium in shear flow is inhibited by adenovirus-mediated gene transfer of IkappaB-alpha. *Blood* 1999; **93**: 3685-3693.

19. Lin SL, Chiang A, Chang D, Ying SY. Loss of mir-146a function in hormone-refractory prostate cancer. *RNA* 2008; **14**: 417-424.

20. Lu LF, Boldin MP, Chaudhry A, Lin LL, Taganov KD, Hanada T *et al*. Function of miR-146a in controlling Treg cell-mediated regulation of Th1 responses. *Cell* 2010; **142**: 914-929.

21. Junker A, Krumbholz M, Eisele S, Mohan H, Augstein F, Bittner R *et al*. MicroRNA profiling of multiple sclerosis lesions identifies modulators of the regulatory protein CD47. *Brain* 2009; **132**: 3342-3352.

22. Abbott NJ, Ronnback L, Hansson E. Astrocyte-endothelial interactions at the blood-brain barrier. *Nat Rev Neurosci* 2006; **7**: 41-53.

23. Gonzalez-Velasquez F, Reed JW, Fuseler JW, Matherly EE, Kotarek JA, Soto-Ortega DD *et al*. Activation of brain endothelium by soluble aggregates of the amyloid-beta protein involves nuclear factor-kappaB. *Curr Alzheimer Res* 2011; **8**: 81-94.

24. Aveleira CA, Lin CM, Abcouwer SF, Ambrosio AF, Antonetti DA. TNF-alpha signals through PKCzeta/NF-kappaB to alter the tight junction complex and increase retinal endothelial cell permeability. *Diabetes* 2010; **59**: 2872-2882.

25. Paris D, Beaulieu-Abdelahad D, Mullan M, Ait-Ghezala G, Mathura V, Bachmeier C *et al*. Amelioration of experimental autoimmune encephalomyelitis by anatabine. *PLoS One* 2013; **8**: e55392.

26. Vig E, Green M, Liu Y, Donner DB, Mukaida N, Goebl MG *et al*. Modulation of tumor necrosis factor and interleukin-1-dependent NF-kappaB activity by mPLK/IRAK. *J Biol Chem* 1999; **274**: 13077-13084.

27. Yoon K, Jung EJ, Lee SR, Kim J, Choi Y, Lee SY. TRAF6 deficiency promotes TNF-induced cell death through inactivation of GSK3beta. *Cell Death Differ* 2008; **15**: 730-738.

28. Bouwmeester T, Bauch A, Ruffner H, Angrand PO, Bergamini G, Croughton K *et al*. A physical and functional map of the human TNF-alpha/NF-kappa B signal transduction pathway. *Nat Cell Biol* 2004; **6**: 97-105.

29. Neuhofer W. Role of NFAT5 in inflammatory disorders associated with osmotic stress. *Curr Genomics* 2010; **11**: 584-590.

30. Buxade M, Lunazzi G, Minguillon J, Iborra S, Berga-Bolanos R, Del Val M *et al*. Gene expression induced by Toll-like receptors in macrophages requires the transcription factor NFAT5. *J Exp Med* 2012; **209**: 379-393.

31. Wang Q, Zhou Y, Rychahou P, Liu C, Weiss HL, Evers BM. NFAT5 represses canonical Wnt signaling via inhibition of beta-catenin acetylation and participates in regulating intestinal cell differentiation. *Cell Death Dis* 2013; **4**: e671.

32. Kleinewietfeld M, Manzel A, Titze J, Kvakan H, Yosef N, Linker RA *et al*. Sodium chloride drives autoimmune disease by the induction of pathogenic TH17 cells. *Nature* 2013; **496**: 518-522.

33. van Rijssel J, Kroon J, Hoogenboezem M, van Alphen FP, de Jong RJ, Kostadinova E *et al*. The Rho-guanine nucleotide exchange factor Trio controls leukocyte transendothelial migration by promoting docking structure formation. *Mol Biol Cell* 2012; **23**: 2831-2844.

34. Adamson P, Etienne S, Couraud PO, Calder V, Greenwood J. Lymphocyte migration through brain endothelial cell monolayers involves signaling through endothelial ICAM-1 via a rho-dependent pathway. *J Immunol* 1999; **162**: 2964-2973.

35. Dhamija S, Doerrie A, Winzen R, Dittrich-Breiholz O, Taghipour A, Kuehne N *et al*. IL-1-induced post-transcriptional mechanisms target overlapping translational silencing and destabilizing elements in IκBζ mRNA. *J Biol Chem* 2010; **285**: 29165-29178.

36. Croft D, McIntyre P, Wibulswas A, Kramer I. Sustained elevated levels of VCAM-1 in cultured fibroblast-like synoviocytes can be achieved by TNF-alpha in combination with either IL-4 or IL-13 through increased mRNA stability. *Am J Pathol* 1999; **154**: 1149-1158.

37. Dunne A, Carpenter S, Brikos C, Gray P, Strelow A, Wesche H *et al*. IRAK1 and IRAK4 promote phosphorylation, ubiquitination, and degradation of MyD88 adaptor-like (Mal). *J Biol Chem* 2010; **285**: 18276-18282.

38. Hu X, Ivashkiv LB. Cross-regulation of signaling pathways by interferon-gamma: implications for immune responses and autoimmune diseases. *Immunity* 2009; **31**: 539-550.

39.   Valastyan S, Weinberg RA. Roles for microRNAs in the regulation of cell adhesion molecules. *J Cell Sci* 2011; **124**: 999-1006.

40.   Suarez Y, Wang C, Manes TD, Pober JS. Cutting edge: TNF-induced microRNAs regulate TNF-induced expression of E-selectin and intercellular adhesion molecule-1 on human endothelial cells: feedback control of inflammation. *J Immunol* 2010; **184**: 21-25.

Figure Legends

Figure 1. miR-146a is increased in CNS microvessels and cultured brain endothelium during inflammation. (**A**) Quantitative RT-PCR analysis of miR-146a in brain endothelial cells isolated by laser capture microdissection from normal appearing whiter matter (NAWM) and MS active lesions (n = 6). Data show the relative abundance of miR-146a normalized to the small nuclear RNA U6B. $P = 0.039$ by paired Student's *t* test. (**B**) Expression of miR-146a in mouse spinal cord microvessels isolated by enzyme digestion was analysed using quantitative RT-PCR. Samples of 3 mice were pooled as one, 9 mice were used for each group. Normal, control Biozzi ABH mice; APP, EAE mice at acute-phase paralysis with a clinical grade score of 4 at day 17; Remission, EAE mice at the first remission stage showing a clinical score of 0.5 and gain of body weight at day 28. Data represent mean ± s.e. n = 3. ***$P < 0.001$ compared with Normal or Remission via ANOVA. (**C**) Representative photomicrographs show by i*n situ* hybridization in combination of immunohistochemistry the expression of miR-146 in PECAM-1 positive spinal cord microvessels of a mouse at day 10 after EAE induction (D10, upper panels) or an EAE-APP mice at day 17 (lower panels) respectively. Left panels show expression of miR-146a (red arrows). Middle panels show immunostaining of endothelium-specific marker PECAM-1 (white arrows). Right panels show merged images to demonstrate colocalization of miR-146a and PECAM-1 (red arrows). Hoechst 33342 labels nuclei (light blue). Scale bar, 25 μm. (**D**) Brain endothelial cell line hCMEC/D3 cells were confluent and left unstimulated or stimulated with 1 ng/ml of TNFα and IFNγ for 0.5, 6, 24, or 48 h. Expression of miR-146a was analyzed with quantitative RT-RCR and normalized to the small nuclear RNA U6B. Values of non-stimulated cells were set as

1. Data represent mean ± s.e. n = 3. *$P < 0.05$, **$P < 0.01$ compared with untreated control via ANOVA.

Figure 2. miR146a modulates Jurkat T cell adhesion to cytokine-stimulated hCMEC/D3 cells. hCMEC/D3 cells in 6-channel slides were transfected with Pre-miR-146a or scrambled Pre-miR, and left untreated or treated with 1 ng/ml TNFα and IFNγ for 24 h. hCMEC/D3 cells were then exposed to CMFDA-labelled Jurkat T cells for 5 min at 0.5 dyn/cm^2. (**A**) Quantitative analysis of effects of Pre-miR-146a on Jurkat T cell adhesion. (**B**) Quantitative analysis of effects of Anti-miR-146a on Jurkat T cell adhesion. (**C**) Quantitative analysis of effects of Pre-miR-146a on primary human T cell adhesion. Data represent mean ± s.e. n = 4 for Jurkat T cell adhesion assay, n = 3 for primary human T cell adhesion assay, experiments for each group at each condition were performed in duplicates. *$P < 0.05$, **$P < 0.01$, ***$P < 0.001$ via Student paired t test.

Figure 3. miR-146a in hCMEC/D3 cells negatively modulates nuclear NF-κB translocation. (**A**) Photomicrographs show NF-κB p65 (RelA) staining in scrambled or Pre-miR-146a transfected hCMEC/D3 cells untreated or treated with 1 ng/ml TNFα and IFNγ for 0.5, 6 and 24 h. Scale bar, 100 μm. (**B**) Effects of Pre-miR-146a on nuclear translocation of NF-κB p65 in hCMEC/D3 cells. Note ectopic expression of miR-146a suppressed nuclear translocation of NF-κB p65 at all three time points. Two-way ANOVA tests of all the time points after cytokine treatment demonstrate significant difference between the Scrambled and Pre-miR-146a groups ($P < 0.001$). One-way ANOVA was used to compare the difference at each time point between the two groups. Data represent mean ± s.e. n = 3, *$P < 0.05$, **$P < 0.01$. (**C**) Effects of

Anti-miR-146a on nuclear translocation of NF-κB p65 in hCMEC/D3 cells. Note that knock-down of miR-146a increased nuclear translocation of NF-κB p65 at all three time points. Two-way ANOVA tests of all the time points after cytokine treatment demonstrate significant difference between the Scrambled and Anti-miR-146a groups ($P < 0.001$). One-way ANOVA was used to compare the difference at each time point between the two groups. Data represent mean ± s.e. n = 3, *$P < 0.05$. (**D**) RelA small interference (siRelA) or small interference control (siControl) was transfected into hCMEC/D3 cells in 12-well plates, 48 h later, cells were left untreated or treated with 1 ng/ml TNFα and IFNγ for 0.5, 6 and 24 h, subject to Western blot for RelA. Note that siRelA suppressed expression of RelA in either untreated or cytokine-stimulated cells at all three time points. siRNA -, siControl; siRNA +, siRelA. (**E**) Decreased expression of RelA prevented Jurkat T cell adhesion to cytokine-stimulated hCMEC/D3 cells. Data represent mean ± s.e. n = 4, *$P < 0.05$, **$P < 0.01$ via Student paired *t* test.

Figure 4. miR-146a targets IRAK1 and TRAF6 to modulate NF-κB activation and Jurkat T cell adhesion. (**A**) Western blot analysis show that over-expression of miR-146a via transfection with Pre-miR-146a repressed the expression of IRAK1 and TRAF6 in hCMEC/D3 cells either unstimulated or cytokine (1 ng/ml TNFα/IFNγ)-stimulated for 0.5, 6 and 24 h. (**B**, **C**) Quantification of protein levels of IRAK1 and TRAF6 via ImageJ. Data represent mean ± s.e. n = 3, *$P < 0.05$, **$P < 0.01$, ***$P < 0.001$ via ANOVA with posthoc comparison and Bonferroni correction. (**D**) Knock-down the expression of IRAK1 via small interference RNA for IRAK1 (siIRAK1) decreased Jurkat T cell adhesion to cytokine-stimulated hCMEC/D3 cells. (**E**) Knock-down the expression of TRAF6 via siTRAF6 down-regulated Jurkat T cell adhesion

to cytokine-stimulated hCMEC/D3 cells. (**F**) Knock-down the expression of IRAK1 and TRAF6 simultaneously decreased Jurkat T cell adhesion to cytokine-stimulated hCMEC/D3 cells. Data represent mean ± s.e. n = 3 - 4, *$P < 0.05$, **$P < 0.05$, ***$P < 0.001$ via ANOVA. (**G**) Statistical analysis the effects of siIRAK1 and siTRAF6 on nuclear translocation of NF-κB. Two-way ANOVA tests of all the time points after cytokine treatment demonstrate significant difference between the siControl and siIRAK1 or siTRAF6 or siIRAK1 + siTRAF6 groups ($P < 0.01$). One-way ANOVA was used to compare the difference with siControl at each time point. Data represent mean ± s.e. n = 3, *$P < 0.05$, **$P < 0.01$.

Figure 5. miR-146a targets NFAT5 and RhoA to modulate NF-κB activation and Jurkat T cell adhesion. (**A**) Western blot analysis show that over-expression of miR-146a via transfection with Pre-miR-146a repressed the expression of NFAT5 and RhoA in hCMEC/D3 cells either untreated or treated with cytokines for 0.5, 6 and 24 h. (**B**, **C**) Quantification of protein levels of NFAT5 and RhoA via ImageJ. Data represent mean ± s.e. n = 3, *$P < 0.05$, **$P < 0.01$, ***$P < 0.001$ via ANOVA with posthoc comparison and Bonferroni correction. (**D**) siNFAT5 decreased Jurkat T cell adhesion to cytokine-stimulated hCMEC/D3 cells. (**E**) siRhoA down-regulated Jurkat T cell adhesion to cytokine-stimulated hCMEC/D3 cells. Data represent mean ± s.e. n = 3 - 4, *$P < 0.05$, **$P < 0.01$, ***$P < 0.001$ via Student paired *t* test. (**F**) Statistical analysis the effects of siNFAT5 and siRhoA on nuclear translocation of NF-κB. Two-way ANOVA tests of all the time points after cytokine treatment demonstrate significant difference between the siControl and siNFAT5 or siRhoA groups ($p<0.001$). One-way ANOVA was used to compare the difference with siControl at each time point. Data represent mean ± s.e. n = 3, **$P < 0.01$, ***$P < 0.001$. (**G**) 3'

UTR luciferase assay demonstrated that miR-146a over-expression led to decreased luciferase activity in hCMEC/D3 cells transduced with lentiviral luciferase vector containing the 3' UTR of RhoA or NFAT5 but no with the corresponding mutated 3' UTR versions. Text box demonstrates a sequence alignment of human miR-146a (hsa-miR-146a) and two target sites in the 3'-UTR of RhoA and one target site in the 3' UTR of NFAT5. Mutated 3'-UTR for RhoA or NFAT5 (mut-RhoA, mut-NFAT5) was performed by replacing the corresponding miR-146a target sites with 4 nucleotides: AAGA. Data represent mean ± s.e. n = 3, *$P < 0.05$ via Student t test.

Figure 6. miR-146a modulated expression of NF-κB-target genes. (**A**) hCMEC/D3 cells were transfected with Pre-miR-146a or scrambled Pre-miR, and left untreated or treated with 1 ng/ml TNFα and IFNγ for 24 h. Expression of two NF-κB-target genes *VCAM1* and *CCL2* was analysed by SYBR green quantitative RT-PCR and normalized to *β-actin*, expressed as relative level to scrambled control. (**B**) hCMEC/D3 cells were transfected with Anti-miR-146a or scrambled Anti-miR, and left untreated or treated with 1 ng/ml TNFα and IFNγ for 24 h. Expression of *VCAM1* and *CCL2* was analysed by SYBR green quantitative RT-PCR and normalized to *β-actin*, expressed as relative level to scrambled control. (**C**) hCMEC/D3 cells were transfected with siIRAK1, siTRAF6 or both or with scrambled siControl, and left untreated or treated with 1 ng/ml TNFα and IFNγ for 24 h. Expression of *VCAM1* and *CCL2* was analysed by SYBR green quantitative RT-PCR and normalized to *β-actin* and expressed as relative levels to siControl. (**D**) hCMEC/D3 cells were transfected with siRelA, siNFAT5 or siRhoA or scrambled siControl, and left untreated or treated with 1 ng/ml TNFα and IFNγ for 24 h. Expression of *VCAM1* and *CCL2* was analysed by SYBR green quantitative RT-PCR and normalized to *β-actin* and expressed as

relative levels to siControl. (**E-I**) Western blot analysis of the levels of VCAM1 protein in hCMEC/D3 cells transfection with Pre-miR-146a (**E**), siIRAK1 or siTRAF6 (**F**), siIRAK1 and siTRAF6 together (**G**), siRhoA or siNFAT5 (**H**), siRelA (**I**), which were left either untreated or treated with 1 ng/ml TNFα/INFγ for 24 h. Data represent mean ± s.e. n = 3, *$P < 0.05$, **$P < 0.01$, ***$P < 0.001$ via ANOVA.

Figure 7. Mechanisms of miR-146a inhibiting NF-κB and T cell adhesion. Pro-inflammatory cytokines TNFα and IFNγ act through their specific receptors on brain endothelial cells, and activate receptor-associated molecules IRAK1 and TRAF6, which then initiate IKKβ- mediated phosphorylation and ubiquitination of IκB, leading to the activation and nuclear translocation of NF-κB (p50/p65). NF-κB initiates transcription of mRNAs including those for CCL2 and VCAM1. CCL2 acts as chemoattractant for T cells, which are attracted and adhere to the brain endothelium through interacting with VCAM1. NF-κB also initiates negative feedback modulators including primary miR-146a. Primary miR-146a is processed by nuclear RNase III enzyme Drosha into Pre-miR-146. Pre-miR-146a is transported to the cytoplasm where it is further processed by cytoplasmic RNase III enzyme Dicer into mature miR-146a. Both NFAT5 and RhoA positively regulate NF-κB activities. Thus miR-146a inhibits NF-κB activation through repressing IRAK1, TRAF6, NFAT5 and RhoA, leading to decreased expression of CCL2 and VCAM1, which results in decreased T cell adhesion to brain endothelium.
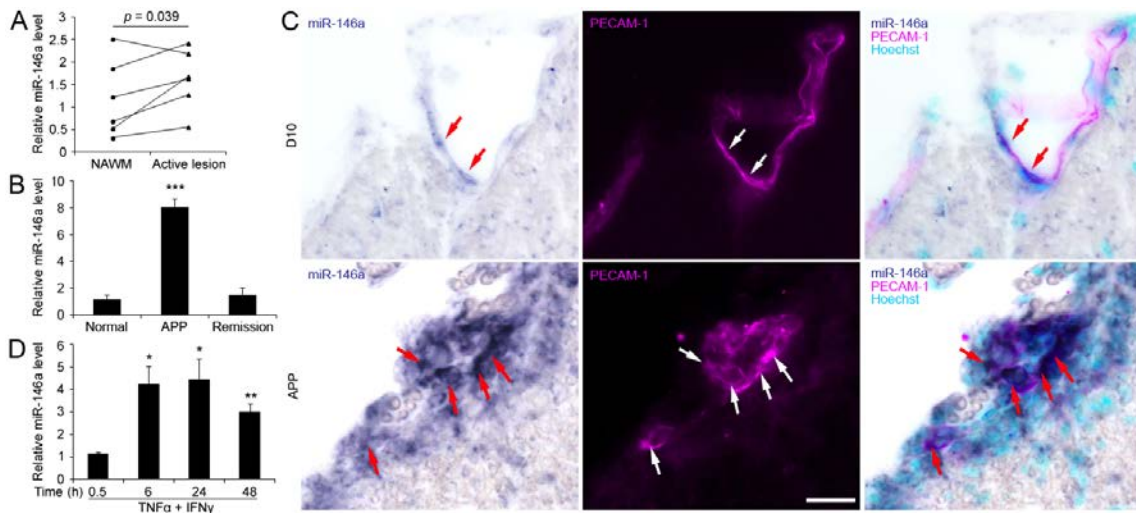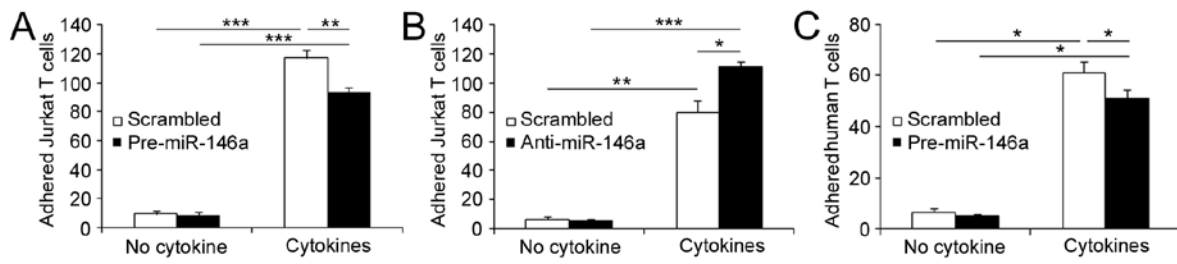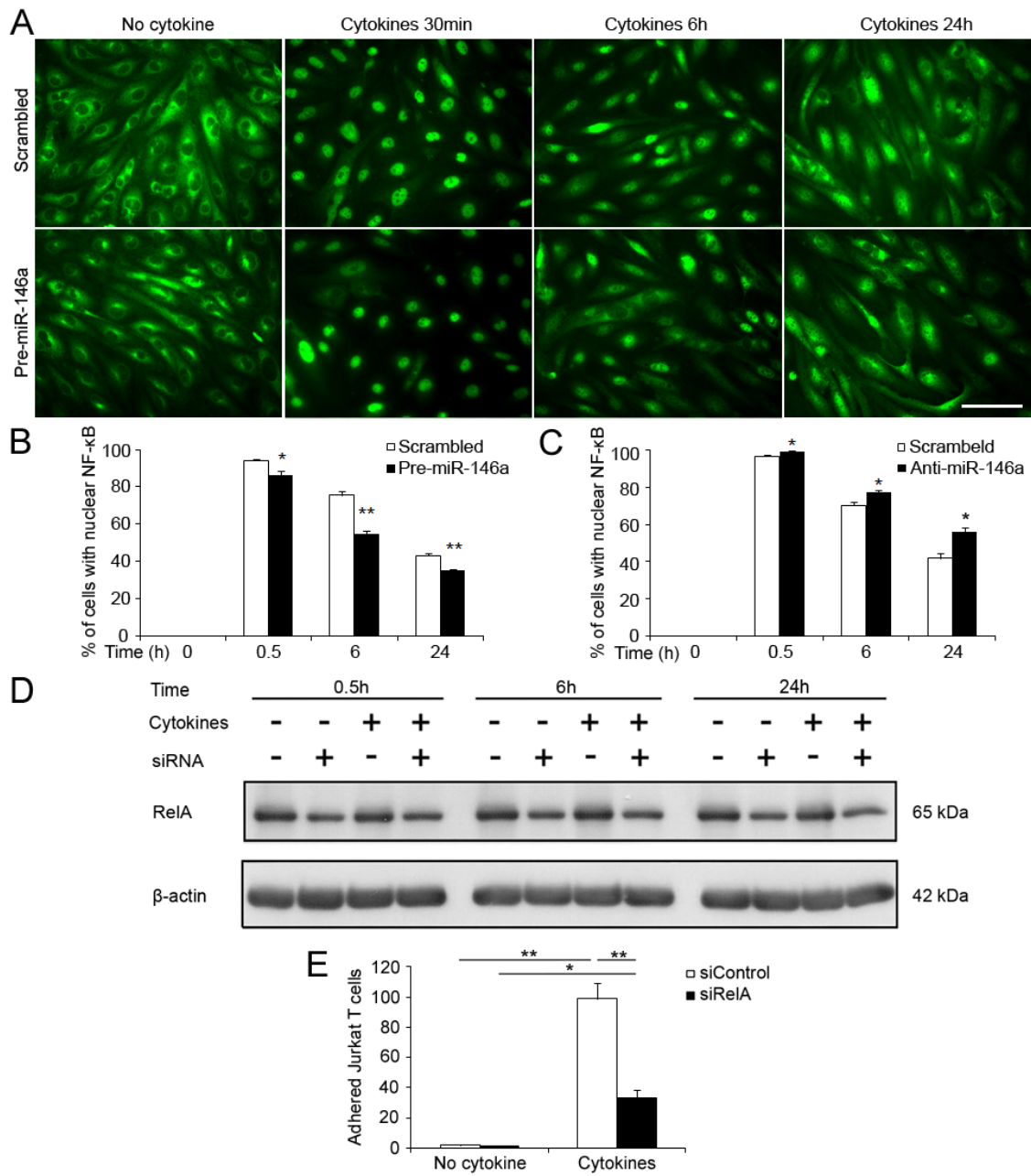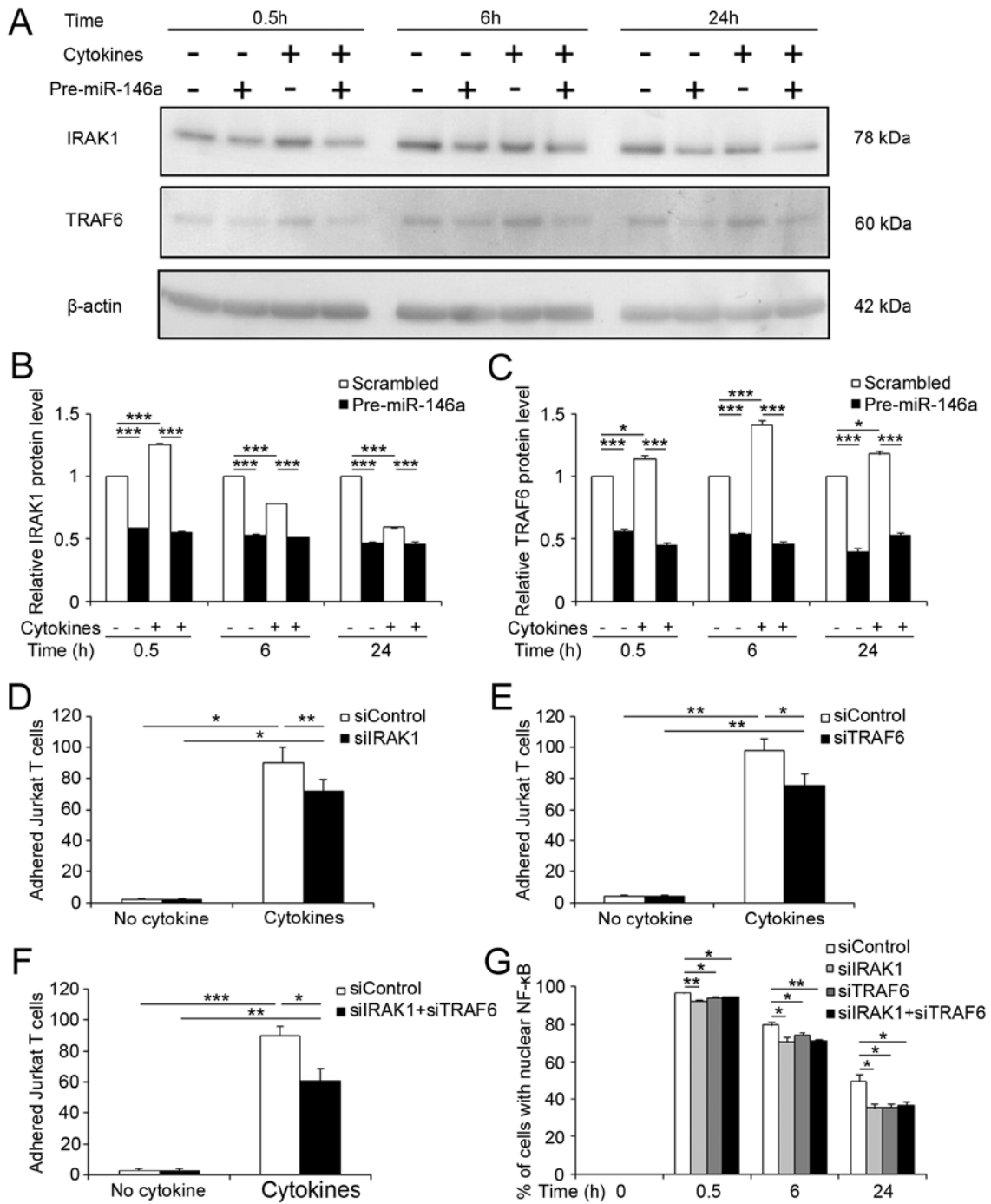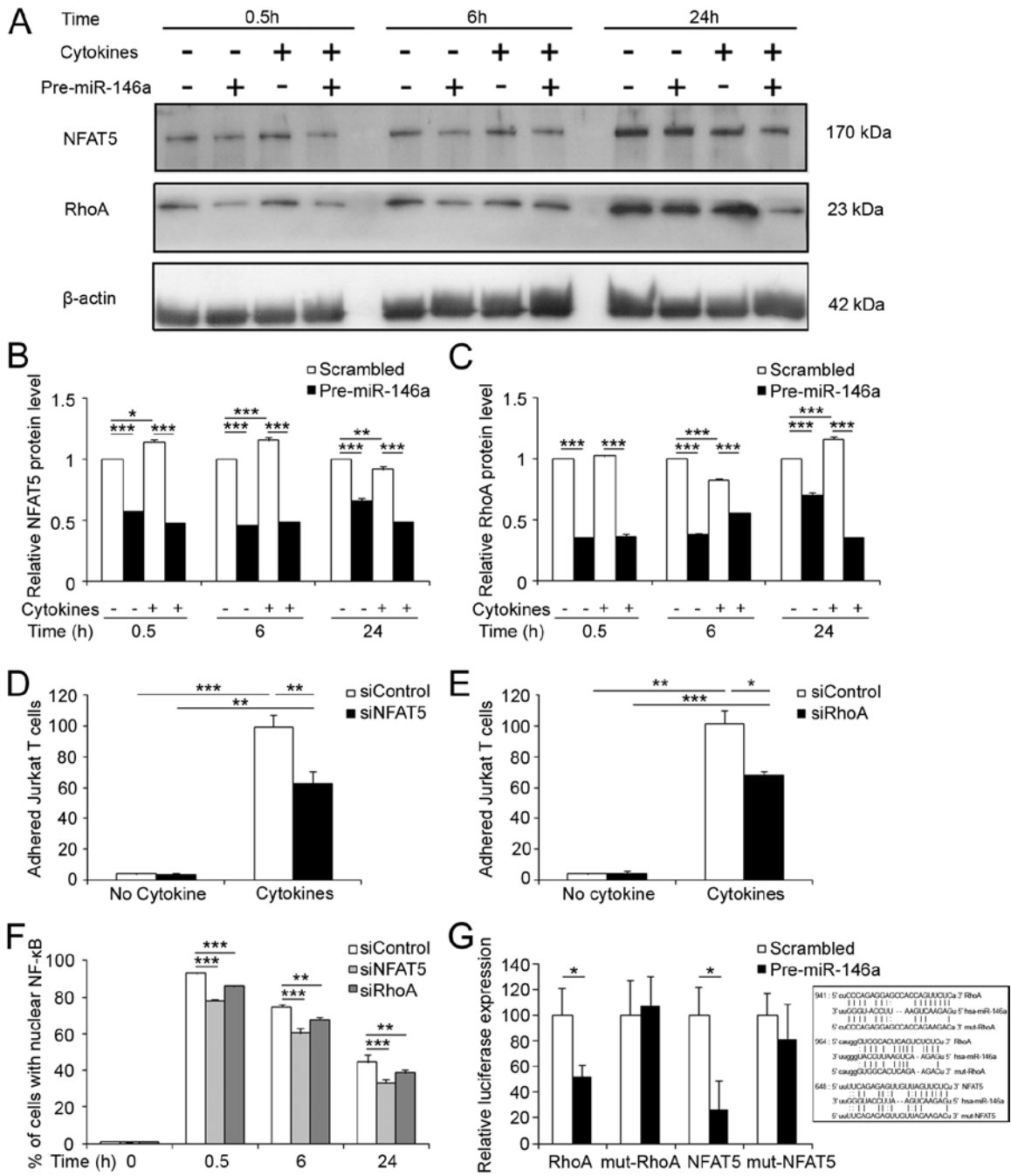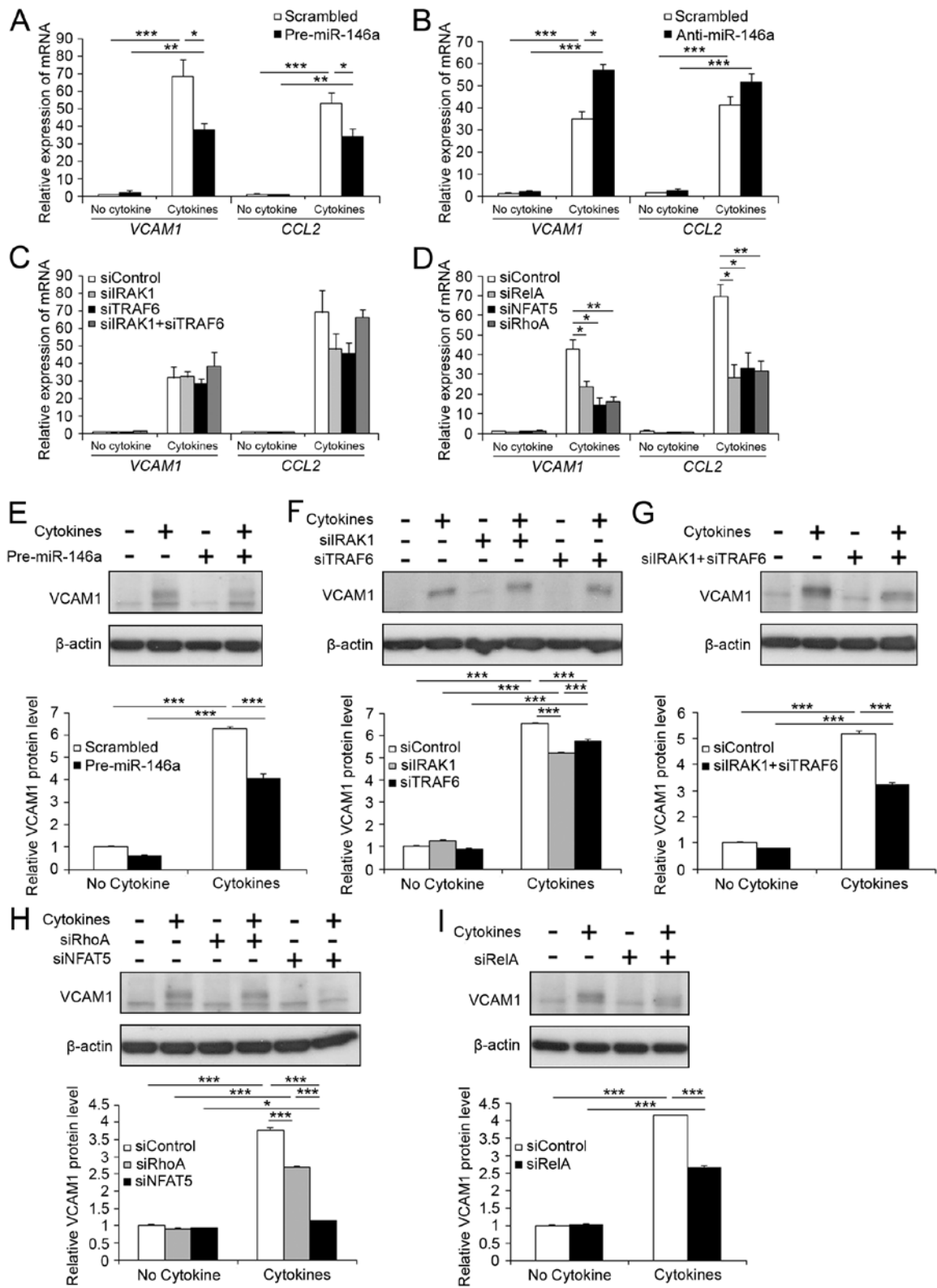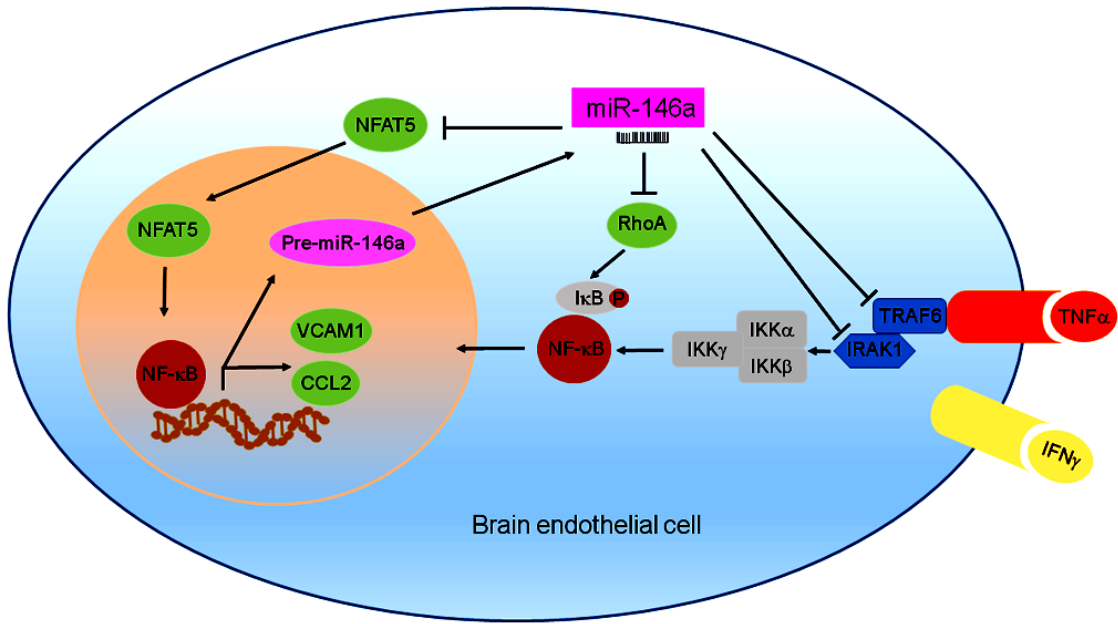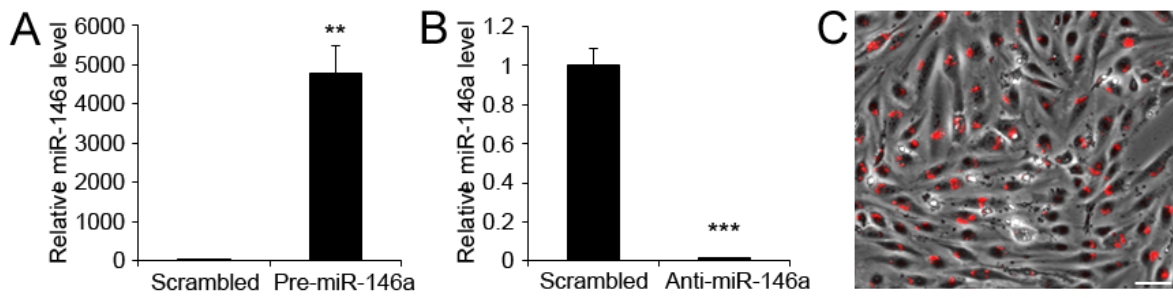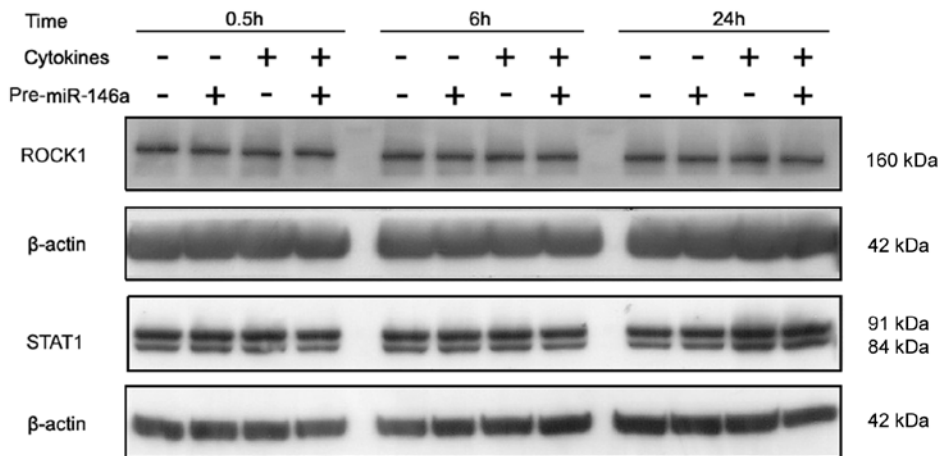
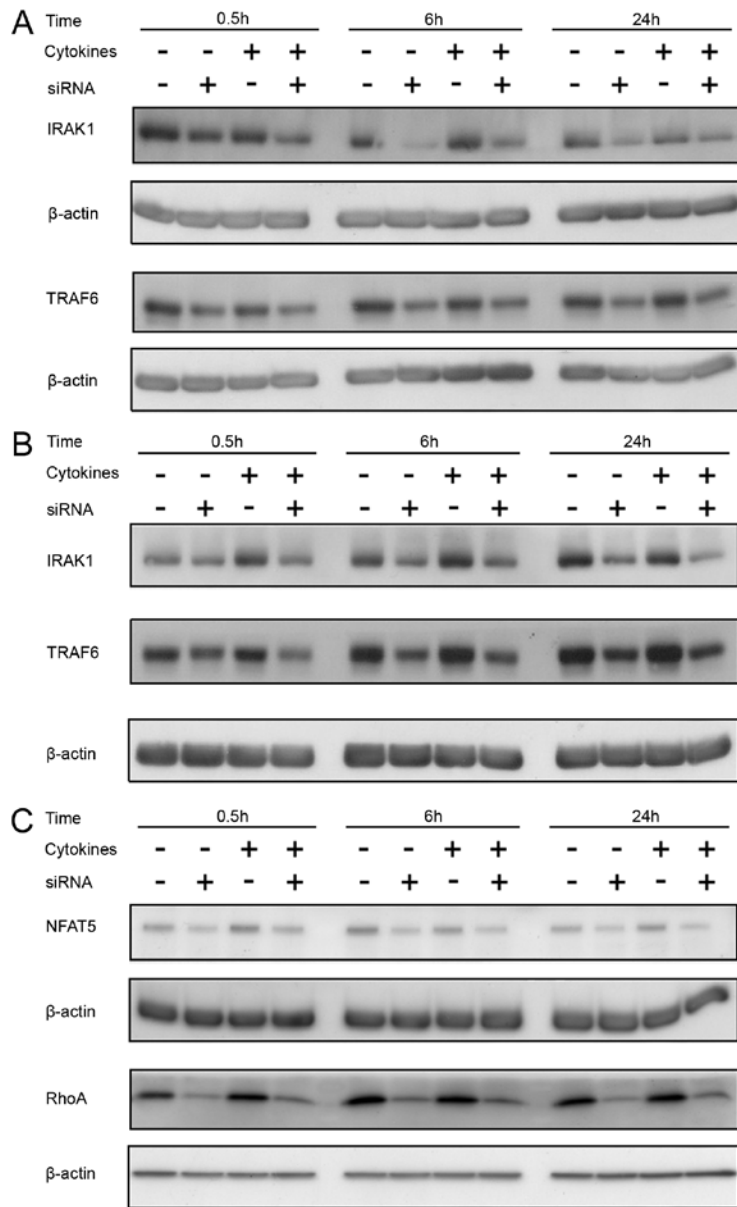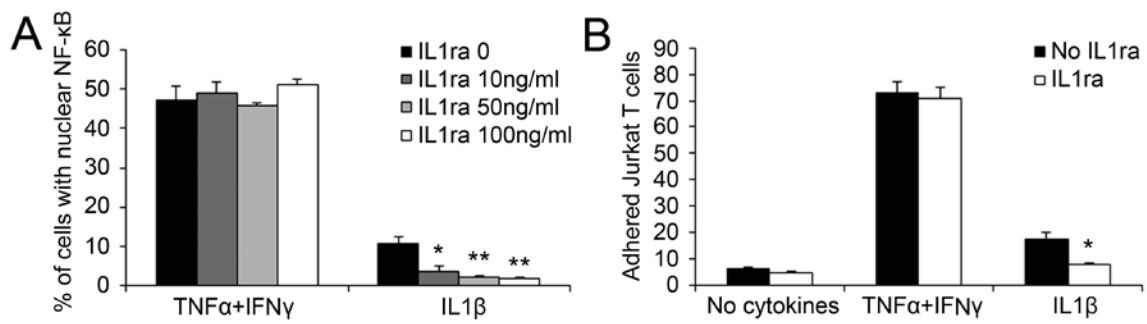Figure 1

Figure 2

Figure 3

Figure 4

Figure 5

Figure 6

Figure 7

Figure S1

Figure S2

A

Time	0.5h	6h	24h
Cytokines	− − + +	− − + +	− − + +
siRNA	− + − +	− + − +	− + − +

IRAK1

β-actin

TRAF6

β-actin

B

Time	0.5h	6h	24h
Cytokines	− − + +	− − + +	− − + +
siRNA	− + − +	− + − +	− + − +

IRAK1

TRAF6

β-actin

C

Time	0.5h	6h	24h
Cytokines	− − + +	− − + +	− − + +
siRNA	− + − +	− + − +	− + − +

NFAT5

β-actin

RhoA

β-actin

Figure S3

A

% of cells with nuclear NF-κB

- IL1ra 0
- IL1ra 10ng/ml
- IL1ra 50ng/ml
- IL1ra 100ng/ml

TNFα+IFNγ   IL1β

B

Adhered Jurkat T cells

- No IL1ra
- IL1ra

No cytokines   TNFα+IFNγ   IL1β

Figure S4